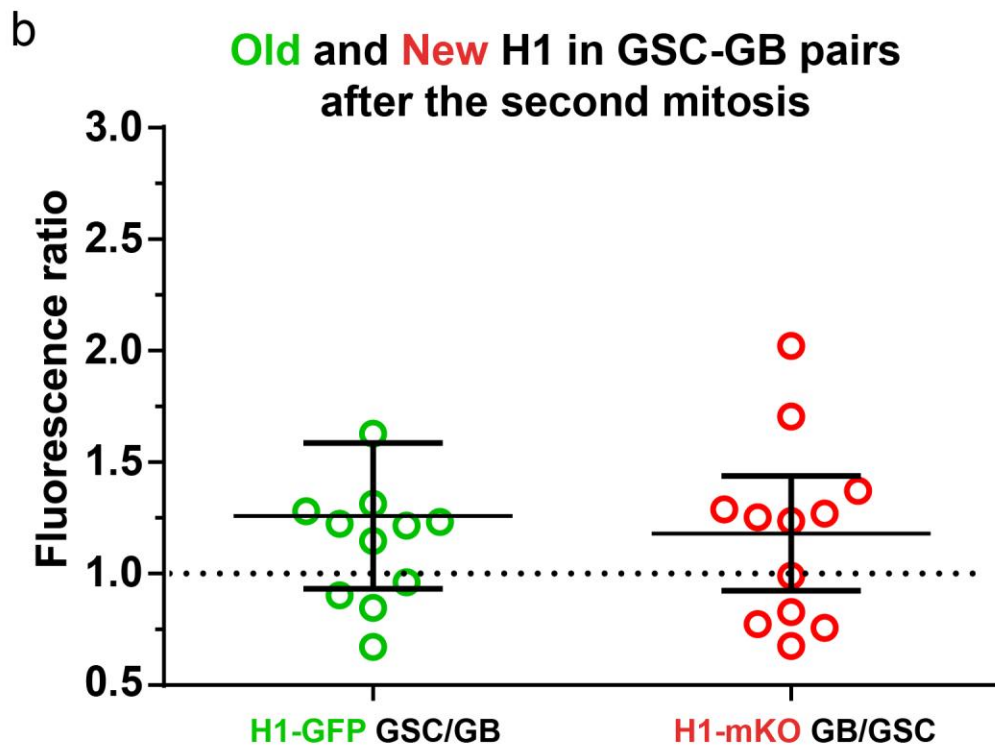
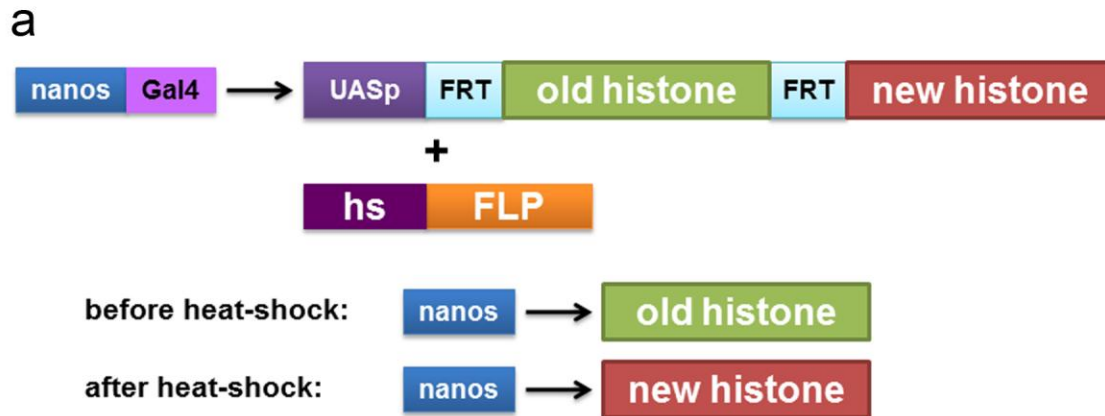


In the format provided by the authors and unedited.

Asymmetric histone inheritance via strand-specific incorporation and biased replication fork movement

Matthew Wooten ¹, Jonathan Snedeker^{1,4}, Zehra F. Nizami^{2,4}, Xinxing Yang^{3,4}, Rajesh Ranjan¹, Elizabeth Urban¹, Jee Min Kim¹, Joseph Gall², Jie Xiao³ and Xin Chen ^{1*}

¹Department of Biology, The Johns Hopkins University, Baltimore, MD, USA. ²Carnegie Institution for Science, Department of Embryology, Baltimore, MD, USA. ³Department of Biophysics and Biophysical Chemistry, Johns Hopkins University School of Medicine, Baltimore, MD, USA. ⁴These authors contributed equally: Jonathan Snedeker, Zehra F. Nizami, Xinxing Yang. *e-mail: xchen32@jhu.edu

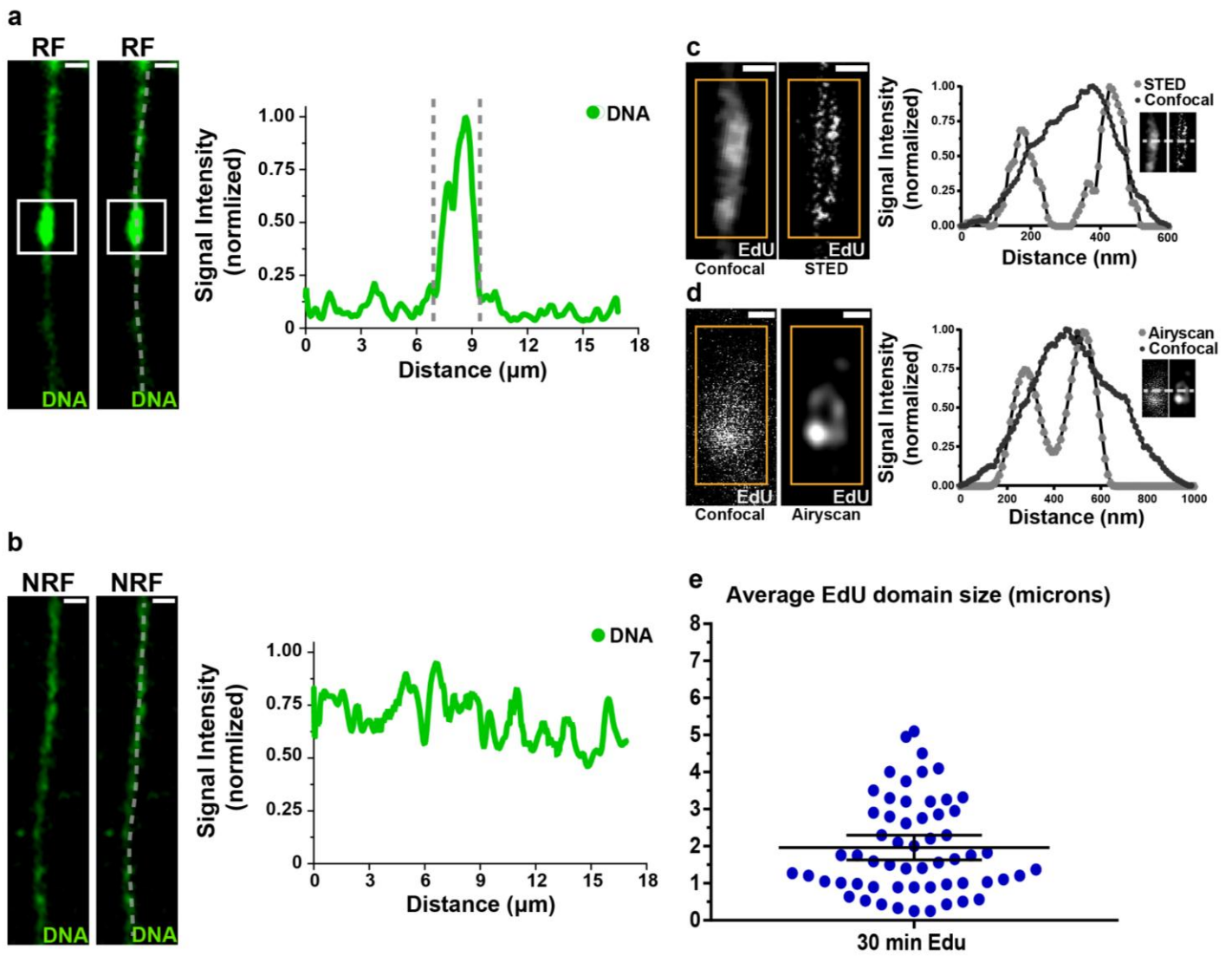


Supplementary Figure 1

H1 inheritance patterns in *Drosophila* GSCs.

(a) A schematic diagram showing the dual color switch design that expresses first preexisting histone and then newly synthesized histone by heat shock treatment, as adapted from². (b) Histone H1 showed overall symmetric inheritance pattern in post-mitotic GSC-

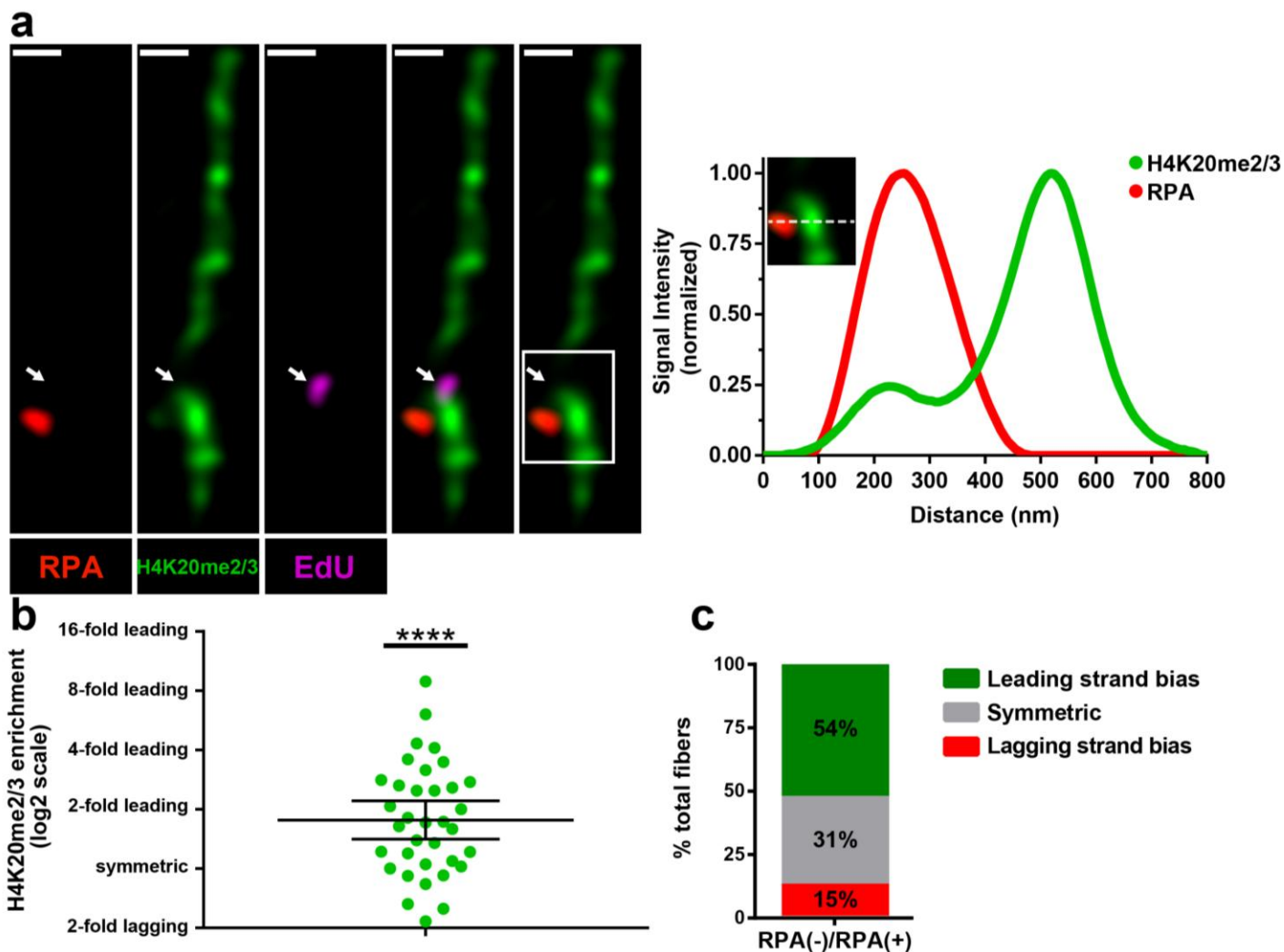
GB pairs (n=12). Individual data points (circles) and mean values are shown. Error bars represent 95% confidence interval. See Supplemental table 1 for details. Neither old H1 nor new H1 is significantly different from the value of 1 based on two-tailed Wilcoxon signed rank-test. H1-GFP GSC/GB ratio = 1.26; H1-mKO GB/GSC ratio = 1.18. H1 old GSC/GB data: Shapiro-Wilk normality test $P = 0.0069$, data not normally distributed. Wilcoxon signed rank-test. Two-tailed test. Sum of signed ranks = 44. $P = 0.0923$. H1 new GB/GSC data: Shapiro-Wilk normality test $P = 0.3147$, data normally distributed. One sample t-test. Two-tailed test $t = 1.546$ $df = 11$. $P = 0.1503$. See Supplementary tables 1 and 2 and online Methods for additional statistical information.



Supplementary Figure 2

Replicating chromatin fibers shown distinct patterns of EdU and DNA label.

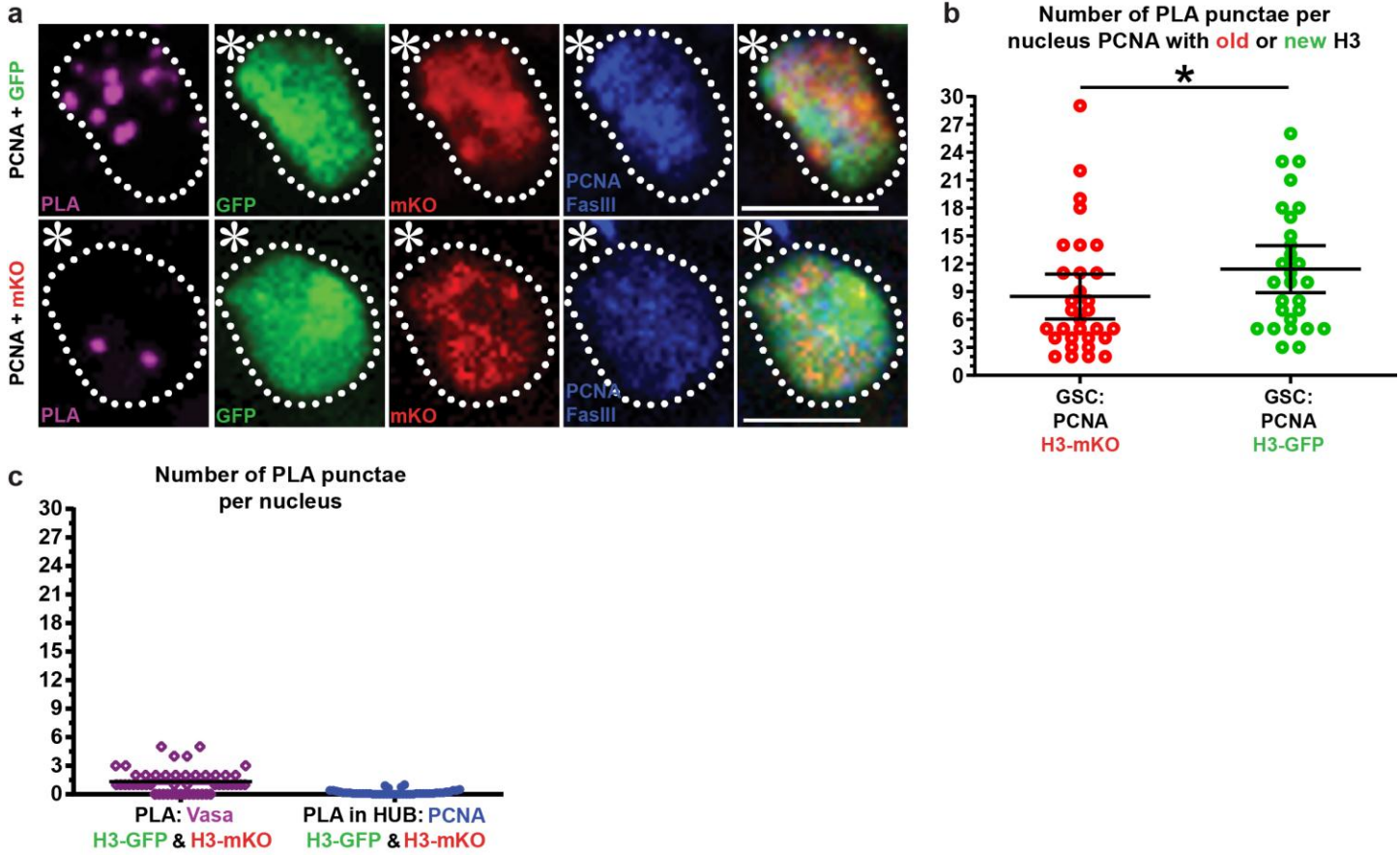
(a) DNA label (DAPI) from RC-derived chromatin fiber shows brighter DNA label (DAPI) in replicating regions (white box). Longitudinal line plot of RC-derived chromatin fiber shows a clear increase in DNA label (DAPI) signal in EdU-positive region, relative to the surrounding EdU-negative region from the same fiber. (b) DNA label (DAPI) from chromatin fiber isolated from non-replicating cells (NRC) in the *Drosophila* adult eye. NRC-derived fibers show uniform DNA label (DAPI). Longitudinal line plot of DNA label (DAPI) intensity in NRC-derived chromatin fiber shows small fluctuations in signal with no significant increases in intensity comparable to those observed in fibers derived from RCs. (c) Confocal versus STED images of EdU signal on replicating chromatin fiber. The EdU-positive region (box with solid orange lines) cannot be resolved into sister chromatids with confocal but can be resolved with STED. Line plot of EdU signal shows a single fiber structure with confocal imaging but a double fiber structure with STED. (d) Confocal versus Airyscan images of EdU signal on replicating chromatin fiber. The EdU-positive region (box with solid orange lines) cannot be resolved into sister chromatids with confocal but can be resolved with Airyscan. Line plot of EdU signal shows a single fiber structure with confocal imaging but a double fiber structure with Airyscan. (e) Quantification of average EdU-positive regions in replicating chromatin fibers. A 30-minute pulse of EdU incorporation yields an average of 1.96 microns; ($n = 58$) of EdU-positive region. Given the estimated average rate of DNA polymerase to synthesize ~ 0.5 - 2.0 kb DNA per minute¹¹, this $2\mu\text{m}$ chromatin fiber reflects approximately 15-60 kb of DNA. Error bars represent 95% confidence interval. See Supplementary table 2 and online Methods for additional statistical information. Scale bar = 500nm for panels a,b,c,d.



Supplementary Figure 3

Old H4 preferentially associate with the leading strand on chromatin fibers.

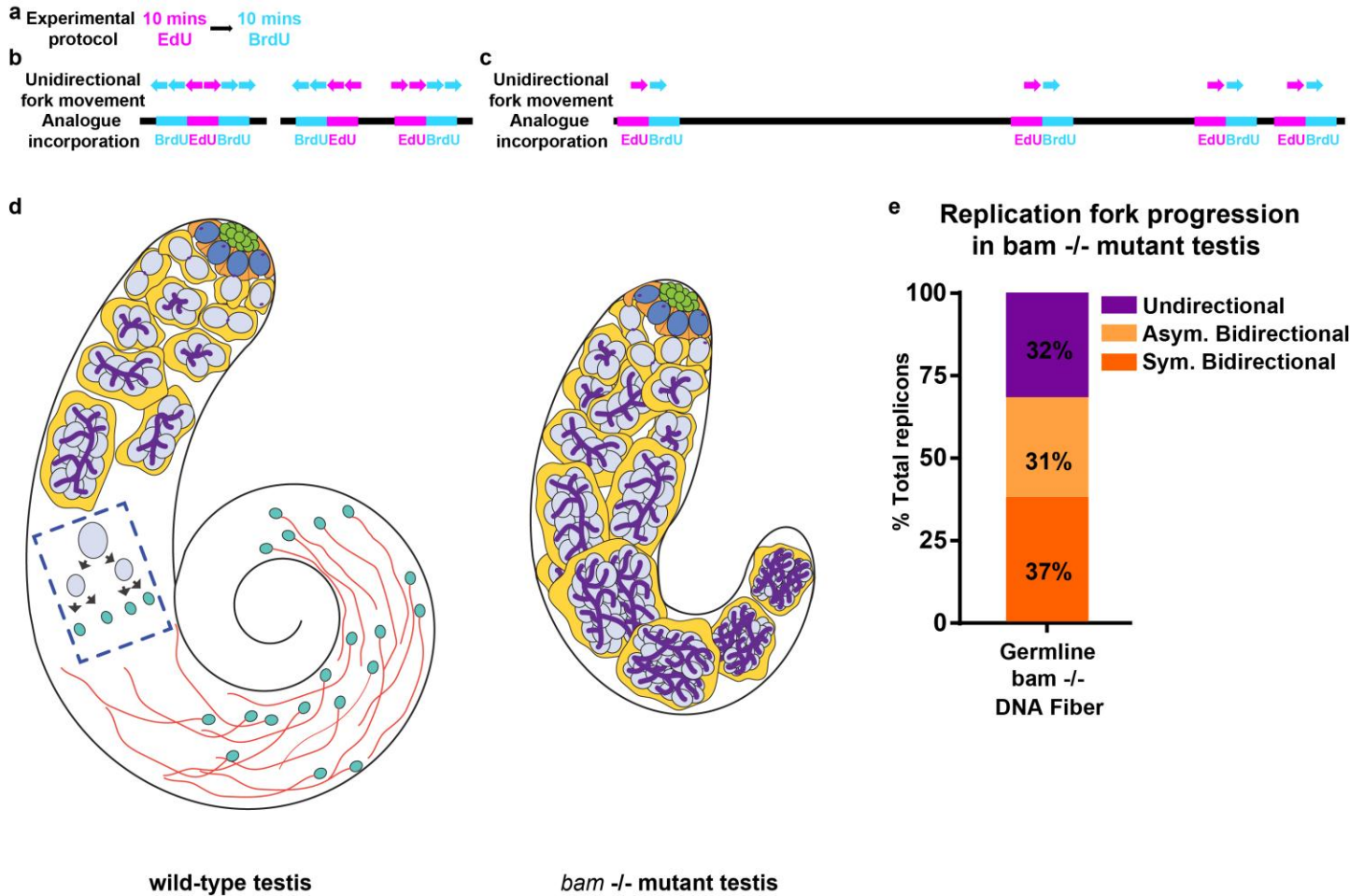
(a) Airyscan image of a chromatin fiber labeled with EdU and H4K20me2/3, and RpA-70. The transition from unreplicated single fiber to replicating double fibers is co-localized with the EdU signal (white arrow). Line plot shows H4K20me2/3 and RpA-70 distribution across replicating region (box with solid white lines). (b) Quantification of the ratio H4K20me2/3 on RpA-70-depleted sister chromatid/ RPA70-enriched sister chromatid. Individual data points (circles) and mean values are shown. Error bars represent 95% confidence in terval. Average fold enrichment= 1.77; n=36 replicating regions from 18 chromatin fibers. Data is significantly different from symmetric (fold enrichment = 0). Y-axis is with log₂ scale. **** $P < 0.0001$, two-tailed one sample t-test. Shapiro-Wilk normality test $P = 0.8594$, data normally distributed. One sample t-test. Two-tailed test $t = 5.149$ $df = 34$. $P < 0.0001$. (d) Classification of RpA-70-labeled sister chromatids into 54% leading strand-enriched (ratio >1.4), 15% lagging strand-enriched (ratio <1.4) and 31% symmetric ($-1.4 < \text{ratio} < 1.4$). Shapiro-Wilk normality test $P = 0.8594$, data normally distributed. One sample t-test. Two-tailed test $t = 5.149$ $df = 34$. $P < 0.0001$. See Supplementary tables 1 and 2 and online Methods for additional statistical information. Scale bar = 500nm for panel a.



Supplementary Figure 4

Proximity ligation assay shows distinct proximity between histones (old versus new) and lagging strand-enriched DNA replication machinery components in GSCs.

(a) A representative GSC showing PLA signals between the lagging strand-enriched component PCNA and new H3-GFP and a representative GSC showing PLA signals between the lagging strand-enriched component PCNA and old H3-mKO. (b) Quantification of the number of PLA puncta per nucleus between PCNA and histones (old *versus* new) in GSCs. Individual data points (circles) and mean values are shown. Error bars represent 95% confidence interval. PLA puncta between PCNA and new H3-GFP: 11.4; n=28; between PCNA and old H3-mKO: 8.5; (n=31), *: $P < 0.05$, based on Mann-Whitney U test. Shapiro-Wilk normality test $P = 0.0013$, data not normally distributed. PCNA + H3-mKO (old H3) GSC Shapiro-Wilk normality test $P = 0.2467$; data normally distributed. Mann-Whitney U two-tailed test: Mann-Whitney U = 297.0. $P = 0.0366$. For PCNA + H3-GFP (new H3) GSC, Shapiro-Wilk normality test $P = 0.0013$, data not normally distributed. For PCNA + H3-mKO (old H3) GSC, Shapiro-Wilk normality test $P = 0.2467$; data normally distributed. Mann-Whitney U two-tailed test: Mann-Whitney U = 297.0. $P = 0.0366$ (c) Quantification of PLA signals in two negative control experiments: first, PLA experiments were performed between histones and a cytoplasmic protein Vasa¹³; second, PLA signals were counted in non-replicating somatic hub cells. Both showed very low signals. Vasa PLA mean = 1.3, n = 52; Hub PLA mean = 0.2; n = 44. Scale bars: 5 μm .



Supplementary Figure 5

DNA fiber dual-pulse experiments in *bam* mutant testis.

(a) A cartoon showing experimental protocol. (b) Predicted unidirectional fork progression result. (c) Unidirectional fork progression pattern from germline-derived chromatin fiber. Multiple replicons show alternation between early label (EdU in magenta) and late label (BrdU in cyan) along one chromatin fiber toward the same direction. DNA label (DAPI) shows continuity between replicons. (d) Cartoon representation of wild-type testes *versus* *bam* mutant testes. (e) Replication patterns in *bam* mutant testis. No category of fork movement (unidirectional, asymmetric bidirectional or bidirectional) shows statistically significant differences from wild-type testes. Chi-squared test: WT Testis vs. *bam* mutant testis. Unidirectional frequency: The chi-square statistic is 0.1169. The p-value is .732432. Asymmetric bidirectional frequency: The chi-square statistic is 0.0821. The p-value is .774529. Symmetric bidirectional frequency: The chi-square statistic is 0.3903. The p-value is .532159.

Supplementary Tables:

Supplemental table 1: Quantification of histone H4, H2A, H2B and H1 with imaging on fixed samples.

H4 Data

Pair #	Old GSC/GB	New GB/GSC		Old H4 SG1/SG1	New H4 SG2/SG1
1	3.95261	0.58145	1	1.01	0.92
2	3.22532	0.85939	2	1.03	0.92
3	3.04916	0.98102	3	0.85	0.82
4	2.95193	1.23534	4	1.05	1.17
5	3.41593	1.05703	5	1.03	0.83
6	5.70124	1.19769	6	1.31	0.77
7	4.86019	1.21894	7	0.76	1.05
8	2.44502	1.43429	8	1.03	1.22
9	1.01334	1.03873	9	1.069	0.98
10	3.15893	0.72547	10	0.92	0.84
11	4.84095	0.75232	11	1.038	1.05
12	5.66219	1.75663	12	0.89	1.22
13	3.21869	0.66236	13	1.026	0.98
14	4.3869	1.1402	14	0.76	0.84
15	4.31614	1.75219	15	1.04	1.05
16	3.65617	0.6908	16	0.925	0.94
17	0.90141	1.15683	17	1.02	0.82
18	0.76087	1.14976	18	0.76	0.95
19	3.6405	0.78695	19	1.04	0.872
20	3.8227	0.57026	20	0.925	1.202
21	1.33704	1.17069	21	1.02	1.147
22	4.53044	1.05605	22	1.016	0.8
23	2.92533	1.07775	23	0.99	1.12
24	3.08045	1.03266	24	1	1.03
25	0.94657	1.28723	25	1.02	0.68
26	4.87384	1.14928	26	1.123	1.38
27	5.97293	2.117	27	1.01	0.93
28	1.39878	0.81597			
29	0.98925	0.98242			

30	0.90328	0.80169			
31	0.86818	1.39117			
32	5.858	1.234			
33	1.1098	1.3476			
34	1.123	1.12			
35	1.02	1.89202			
36	1.12176	0.88736			
37	1.32	0.98			
38	1.39	1.01			
39	1.87	1.38			
40	0.98	1.05			
41	0.99	1.25			
42	1.8654	1.3453			
43	2.261	1.35			
44	2.56	1.11			

H2A
Data

Pair #	Old H2A GSC/GB	New H2A GB/GSC	Pair #	Old H2A SG1/SG2	New H2A SG2/SG1
1	0.97526	0.98053	1	1.08853	1.04377
2	0.96884	0.96606	2	1.01652	1.01619
3	0.96911	0.94179	3	0.94226	0.97414
4	1.23228	1.63322	4	1.06756	0.91538
5	1.02585	1.04176	5	1.0099	0.96247
6	1.05326	0.9991	6	1.04282	0.94673
7	0.96981	1.1862	7	1.01932	0.95029
8	0.79768	1.35798	8	1.22233	0.88543
9	1.07599	1.12273	9	0.99573	1.01997
10	1.12152	0.90102	10	0.93019	1.00929
11	1.06131	1.10325	11	0.93179	0.93155
12	0.9124	1.06645	12	0.98612	0.97988
13	0.80183	1.20448	13	0.92509	1.04502
14	1.07001	0.98794	14	1.01963	1.1036
15	0.72145	1.24709	15	1.03505	1.11993
16	1.33841	1.24652	16	0.96955	0.97257
17	0.89897	1.15451	17	0.97267	1.03535

18	1.15294	1.01967	18	1.02315	1.16413
19	1.05437	0.82361	19	0.97885	1.1532
20	0.92081	1.0273	20	1.05542	1.02936

H2B
Data

Pair #	Old H2B GSC/GB	New H2B GB/GSC	Pair #	Old H2B SG1/SG2	New H2B SG2/SG1
1	0.81528	1.14988	1	1.0688	1.0368
2	0.91081	1.0871	2	0.83419	1.01759
3	0.99257	0.90021	3	1.01062	0.86112
4	0.97881	1.0615	4	1.04684	1.05203
5	1.17406	0.82182	5	0.91619	0.87483
6	0.87227	1.36065	6	0.97398	1.32672
7	1.16273	0.82736	7	1.22016	0.74991
8	1.17149	1.60111	8	1.00927	0.96835
9	1.03788	0.91736	9	0.9475	1.17024
10	0.99784	0.92363	10	0.85415	1.17491
11	0.89508	1.28192	11	1.17214	0.85816
12	0.9595	1.47957	12	1.0834	0.84516
13	1.23109	1.12747	13	1.07626	0.92324
14	0.8087	1.21191	14	1.02165	0.9204
15	1.04669	1.14397	15	0.86262	1.17237
16	0.84908	1.45383	16	1.02649	1.93949
17	1.05537	1.12127	17	1.02344	0.97242
18	1.01445	1.16539	18	0.92834	0.85676
19	0.9126	1.30627	19	0.90029	1.91883
20	1.02197	0.86291	20	1.06675	1.14407
21	1.20262	1.19143	21	1.09933	0.66265
22	0.88773	2.07111	22	1.15347	0.59781
23	0.9908	0.88569	23	0.98268	1.37432
24	0.91825	0.8915	24	0.8445	1.20599
25	0.91222	1.38431	25	1.03604	0.85231
26	0.86945	1.11417	26	1.06476	0.94824
27	1.1907	1.01954	27	0.88406	1.05915
28	0.89128	1.1297	28	1.09301	0.9983
29	1.04879	0.9498	29	1.08044	1.30052

30	1.21441	0.84858	30	1.22264	1.0443
31	0.93556	1.3278	31	1.03789	1.10251
32	0.84399	1.59379	32	1.12615	0.97758
33	1.01138	1.16682	33	0.81355	0.91765
34	0.90725	1.46625	34	1.08318	0.96847
35	0.89401	1.03343	35	0.90433	1.0319
36	1.11016	1.90552	36	1.01597	1.01317
37	0.91736	1.47624			
38	0.96429	1.28084			
39	0.97663	2.04853			
40	0.9693	0.89053			

H1
Data

Pair#	Old H1 GSC/GB	New H1 GB/GSC
1	1.23162	1.23631
2	1.31383	1.37178
3	1.28099	1.28898
4	2.6868	2.02088
5	1.2147	0.67617
6	0.96056	0.99023
7	1.14701	1.70528
8	1.62913	1.25233
9	0.67269	0.77294
10	0.84621	0.75771
11	1.22312	1.26967
12	0.90353	0.82814

Table 2: Averages and 95% confidence intervals for all datasets

H4 data summary:

Data set (figure):	Average	95% Confidence interval
H4-GFP GSC/GB ratio (Figure 1)	2.73	$2.24 \leq x \leq 3.23$

H4-mKO GB/GSC ratio (Figure 1)	1.13	$1.03 \leq x \leq 1.22$
H4-GFP SG1/SG2 ratio (Figure 1)	0.99	$0.94 \leq x \leq 1.03$
H4-mKO SG2/SG1 (Figure 1)	0.98	$0.92 \leq x \leq 1.05$
H2A-GFP GSC/GB ratio (Figure 2)	1.00	$0.94 \leq x \leq 1.08$
H2A-mKO GB/GSC ratio (Figure 2)	1.10	$1.02 \leq x \leq 1.19$
H2A-GFP SG1/SG2 ratio (Figure 2)	1.01	$0.98 \leq x \leq 1.04$
H2A-mKO SG2/SG1 ratio (Figure 2)	1.01	$0.98 \leq x \leq 1.05$
H2B-GFP GSC/GB ratio (Figure 2)	0.99	$0.95 \leq x \leq 1.03$
H2B-mKO GB/GSC ratio (Figure 2)	1.21	$1.11 \leq x \leq 1.31$
H2B-GFP SG1/SG2 ratio (Figure 2)	1.01	$0.98 \leq x \leq 1.05$
H2B-mKO SG2/SG1 (Figure 2)	1.05	$0.96 \leq x \leq 1.14$
H1-GFP GSC/GB ratio (Supplementary figure 1)	1.26	$0.93 \leq x \leq 1.59$
H1-mKO GB/GSC ratio (Supplementary figure 1)	1.18	$0.92 \leq x \leq 1.44$
30-minute pulse of EdU incorporation length (Sup. fig. 2)	1.96 μ m	$1.63 \leq x \leq 2.30$
Quantification of old H2A on sister chromatids (Figure 4)	1.36	$1.29 \leq x \leq 1.44$
Quantification of old H3 on sister chromatids (Figure 4)	2.41	$2.03 \leq x \leq 2.79$
Quantification of new H2A on sister chromatids (Figure 4)	1.24	$1.13 \leq x \leq 1.36$
Quantification of new H3 on sister chromatids (Figure 4)	1.94	$1.62 \leq x \leq 2.27$
H3K27me3 fold-enrichment on RPA70-enriched sister (Figure 5)	3.20	$2.30 \leq x \leq 4.52$
H3K27me3 fold-enrichment on PCNA-enriched sister (Figure 5)	2.04	$1.60 \leq x \leq 2.50$

H3K4me3 fold enrichment on RPA70 enriched sister	1.77	$1.41 \leq x \leq 2.21$
PLA puncta between ligase and new H3-mKO in GSCs (Figure 6)	26.5	$23.0 \leq x \leq 30.0$
PLA puncta between ligase and old H3-GFP in GSCs (Figure 6)	18.5	$16.0 \leq x \leq 21.5$
PLA puncta between ligase and new H3-mKO in SGs (Figure 6)	16.7	$13.0 \leq x \leq 20.3$
PLA puncta between ligase and old H3-GFP in SGs (Figure 6)	21.9	$18.7 \leq x \leq 25.1$
PLA puncta between PCNA and new H3-mKO in GSCs (Figure 6)	12.3	$10.2 \leq x \leq 14.4$
PLA puncta between PCNA and old H3-GFP in GSCs (Figure 6)	7.2	$5.8 \leq x \leq 8.6$
PLA puncta between PCNA and new H3-mKO in SGs (Figure 6)	8.3	$7.0 \leq x \leq 9.7$
PLA puncta between PCNA and old H3-GFP in SGs (Figure 6)	7.6	$6.3 \leq x \leq 8.9$
PLA puncta between ligase and old H3-mKO in GSCs (sup. fig. 4)	8.5	$6.1 \leq x \leq 10.9$
PLA puncta between ligase and new H3-GFP in GSCs (sup. fig. 4)	11.4	$8.9 \leq x \leq 14.0$
PLA puncta between old or new histones and Vasa (sup. fig. 4)	1.3	$1.0 \leq x \leq 1.7$
PLA puncta in hub cells in all experiments (sup. fig. 4)	0.2	$0.1 \leq x \leq 0.3$